

## Article

# Spatiotemporal Evolution of Territorial Spaces and Its Effect on Carbon Emissions in Qingdao City, China

Jiali He <sup>†</sup> , Xiangfei Liu <sup>†</sup>, Xuotong Wang , Xueyang Li, Linger Yu and Beibei Niu <sup>\*</sup> 

College of Resources and Environment, Shandong Agricultural University, Tai'an 271018, China; jialihe@ldy.edu.rs (J.H.); 2023110209@sda.u.edu.cn (X.L.); 2023110211@sda.u.edu.cn (X.W.); 2023120264@sda.u.edu.cn (X.L.); lingeryu@ldy.edu.rs (L.Y.)

\* Correspondence: bbnwhu@sda.u.edu.cn; Tel.: +86-13220-628-537

<sup>†</sup> These authors contributed equally to this work.

**Abstract:** Land use change has always been a significant factor affecting global carbon emissions. Dissecting the characteristics of territorial space evolution and its impact on carbon emissions is crucial for developing low-carbon-oriented territorial space optimization and governance strategies. This paper calculates the carbon emissions associated with territorial spaces in Qingdao from 2000 to 2020, utilizing land use data alongside various statistical data. Based on the accounting results, the evolution characteristics of territorial spaces and their corresponding carbon emissions, as well as the carbon transition dynamics resulting from space transfer, are analyzed. A carbon transition decomposition formula is then proposed to quantify the differential and spatially heterogeneous impacts of changes in space types and socio-economic development on emissions. The results indicate that: (1) the evolution of territorial spaces in Qingdao during 2000–2020 is characterized by an expansion of living space and a contraction of production and ecological spaces; (2) net carbon emissions rose from  $313.98 \times 10^4$  tons to  $1068.58 \times 10^4$  tons, with urban production space contributing the most (69.96% in 2020) due to its significantly high emission density. The spatial distribution of carbon emissions exhibited a stable “northwest–southeast” pattern, with increased dispersion and weakened directionality; (3) the transformation of territorial spaces promoted carbon emissions in Qingdao, with the conversion of urban production space to other uses yielding the most favorable carbon transitions, while the expropriation of agricultural production spaces for urban production and residents’ living has resulted in the most detrimental carbon transitions; (4) socio-economic development shapes the overarching pattern of regional emission density changes, whereas space transfers account for local variations. This paper also identifies priorities for spatial optimization and key sectors for emission reduction. The findings contribute to a deeper understanding of the carbon emission consequences of territorial space transformation in Qingdao, thereby providing valuable insights for regional spatial planning and optimization aimed at promoting low-carbon development.



**Citation:** He, J.; Liu, X.; Wang, X.; Li, X.; Yu, L.; Niu, B. Spatiotemporal Evolution of Territorial Spaces and Its Effect on Carbon Emissions in Qingdao City, China. *Land* **2024**, *13*, 1717. <https://doi.org/10.3390/land13101717>

Academic Editors: Xuechao Wang, Weize Song and Yingjie Li

Received: 15 August 2024

Revised: 15 October 2024

Accepted: 16 October 2024

Published: 20 October 2024



**Copyright:** © 2024 by the authors. Licensee MDPI, Basel, Switzerland. This article is an open access article distributed under the terms and conditions of the Creative Commons Attribution (CC BY) license (<https://creativecommons.org/licenses/by/4.0/>).

**Keywords:** carbon emission; territorial space; carbon transition flux; space transfer; Qingdao city

## 1. Introduction

Land use and land use change considerably alter the structure, process, and function of ecosystems, thereby affecting carbon exchange between the land and the atmosphere [1]. With increased population and urbanization, unsustainable land use practices (such as excessive agricultural cultivation, industrial construction, urban sprawl, etc.) over the past few decades have significantly diminished the land’s carbon sequestration ability and increased carbon emissions [2–4]. Human activity is primarily concentrated in urban areas, carbon emissions from which amounted to 67 to 72% of total global emissions in 2020 [5]. As the carrier of human production and life, the allocation and pattern of land use can indirectly affect anthropogenic carbon emissions by constraining the distribution and intensity of human activities, and the carbon fluxes considering land transitions can vary at

a higher magnitude [6]. These point out the great potential of urban land management and spatial adjustment for carbon reduction. In China, land space is divided into urban space, agricultural space, and ecological space to balance urban development, food security, and ecological protection [7]. Understanding the evolution characteristics of regional territorial spaces and their effects on carbon emissions is crucial for optimizing spatial layouts and achieving low-carbon sustainable development.

Research on carbon emissions associated with land use has gained significant attention in recent years, with two mainstream research perspectives [8,9]. One views the land as ecosystems, focusing on the changes in carbon stocks and emissions related to biomass, dead organic matter, and soil carbon caused by land use and land use change, which are mainly related to deforestation, afforestation, logging and forest degradation, shifting cultivation, and regrowth of forests [10]. Key research topics include estimating carbon fluxes [11], identifying the contributions of different regions and land use change categories to global historical and contemporary emissions [6], and exploring land management strategies to achieve net-zero emissions [12]. Another perspective sees land as a carrying space for emission activity, emphasizing the accounting and analysis of emissions, typically from energy consumption, industrial processes, waste, etc., occurring in different land spaces. Related studies primarily concentrate on carbon emission accounting and forecasting [13–15], spatiotemporal differentiation characteristics [16], the emission effect of land use changes [17,18], and driving mechanisms and influencing factors [19,20], as well as low-carbon optimization and planning [21]. Carbon emission accounting serves as a critical foundation for analyzing emissions characteristics and informing policy decisions. The majority of studies on accounting for anthropogenic emissions and removals occurring on various land spaces follow the IPCC Guidelines for National Greenhouse Gas Inventories [22]. From the research scale perspective, related studies have been conducted at various levels, including global, national, provincial, urban agglomeration, and key city scales; however, the predominant focus remains on medium to macro scales [23]. The ultimate goal of these studies is to establish a scientific foundation for land management or planning, ultimately facilitating carbon reduction efforts.

Under the strategic background of high-quality development and ecological civilization construction, China has initiated a comprehensive integration of various planning frameworks and has progressively established a cohesive national spatial planning system since 2014 [24]. Consequently, the issue of carbon emissions associated with territorial spaces has garnered increasing attention from scholars. Territorial space refers to a land function classification system that organizes land use types with analogous functions into categories such as urban, agricultural, and ecological spaces [7]. Therefore, the current research on carbon emissions in relation to territorial space is mainly based on the correspondence between territorial spaces and land use types and is performed according to the research framework of land use carbon emissions. In addition, the mainstream research route is to conduct emission forecasting or low-carbon zoning management based on carbon emission accounting and spatiotemporal pattern analysis [23,25,26].

Investigations into the effects of land use change on carbon emissions have been approached from various angles. Some studies examined the spatiotemporal effects of land use change on carbon emissions through land use simulations and predictive modeling under diverse scenarios [27]. Some employed decomposition analysis to elucidate the influence of alterations in land use structure on carbon emissions [28,29]. In addition, there is also research focused on the effects of changes in land use characteristics, such as land use intensity and land urbanization, on carbon emissions with various econometric methods [30]. These studies enhance our comprehension of the overall implications of land use patterns, structures, intensities, and other characteristics on carbon emissions. However, there is still a lack of quantitative descriptions of carbon emission flows caused by regional land use transfer processes. The land use transfer matrix and transfer map serve as effective tools to illustrate the primary pathways, locations, and extents of land use transfers over a specified timeframe. Based on this, it is feasible to quantify the carbon transfer flux

resulting from various transfer pathways, which enables a more comprehensive analysis of the direction and magnitude of the effect of spatial transfer on carbon emissions [31]. However, the impact of land use transfer on carbon emissions is a joint effect of land use type changes and socio-economic development, and the distinct impacts of these factors across different periods and transfer paths have yet to be effectively decomposed and spatially located.

China has incorporated “carbon peaking and carbon neutrality” into the overall layout of ecological civilization construction, and low-carbon-oriented territorial space utilization is a new requirement for urban advancement. Qingdao, as the economic center of Shandong Province, functions as a critical node within the New Asia–Europe Continental Bridge Economic Corridor and serves as a strategic city for maritime collaboration. The city’s rapid urbanization, industrialization, and substantial alterations in land use have resulted in a notable increase in carbon emissions [32]. As a low-carbon pilot city, Qingdao’s potential for carbon reduction has been extensively examined from various perspectives, including energy structure, energy efficiency, solid waste management, and resident behavior [33–35]. However, limited attention has been paid to the impact of territorial space changes on carbon emissions in Qingdao, particularly regarding the differential impacts of space type changes and socio-economic development during the process of territorial space transformation. Consequently, this study aims to analyze Qingdao’s territorial space and its associated carbon emissions from 2000 to 2020, utilizing the established relationship between different territorial space types and carbon emission sectors. The specific objectives of this research are: (1) to characterize the spatiotemporal evolution characteristics of territorial spaces and carbon emissions in Qingdao from 2000 to 2020; (2) to identify the features of carbon transitions resulting from territorial space transformations; and (3) to differentiate the impacts of changes in space types and socio-economic factors during the process of territorial space transfer. The findings of this study can provide a scientific foundation and strategic guidance for the optimization and governance of low-carbon-oriented territorial spaces.

## 2. Materials and Methods

### 2.1. Study Area

Qingdao is located in the southern part of the Shandong Peninsula, bordering the Yellow Sea to the east. It has administrative jurisdiction over 10 districts, encompassing an area of 11,293 km<sup>2</sup> between latitudes 35°35′~37°09′ N and longitudes 119°30′~121°00′ E (see Figure 1). The topography of Qingdao is characterized by elevated terrain in the eastern part and lower elevations in the west, with uplands flanking the north and south and a central depression. The region experiences a temperate monsoon climate, influenced by its marine surroundings. This advantageous geographical setting enhances the abundance and variety of natural resources within the study area.

As the core city of the Shandong Peninsula urban agglomeration, Qingdao has witnessed a continuous increase in urbanization and industrial development in recent years, leading to significant alterations in the spatial configuration of land use, as well as the density and distribution of carbon emissions. Nowadays, a pronounced focus on low-carbon development and the optimization of territorial space is reflected in both policy frameworks and ongoing urban initiatives. Consequently, it is imperative to investigate the evolution of territorial space and its implications for carbon emissions.

### 2.2. Methods

This study aims to analyze the evolution of territorial spaces and its impact on carbon emissions in Qingdao City, and Figure 2 depicts the general technical route. We first established the matching relationship between land use types and territorial space types. Based on this relationship and alongside land use data, we mapped the distribution of territorial spaces in Qingdao from 2000 to 2020. Subsequently, we analyzed the spatiotemporal variations of territorial space through area statistics and transfer matrices. Next, we

conducted carbon emission accounting and allocated the emissions from various sectors to their corresponding carrying spaces. Through total changes, density changes, and standard deviation ellipses, we investigated the evolutionary characteristics of carbon emissions. Finally, based on carbon transition flux and decomposition of changes in carbon emission density, we differentiated the impacts of changes in space types and socio-economic factors during the process of territorial space transfer.

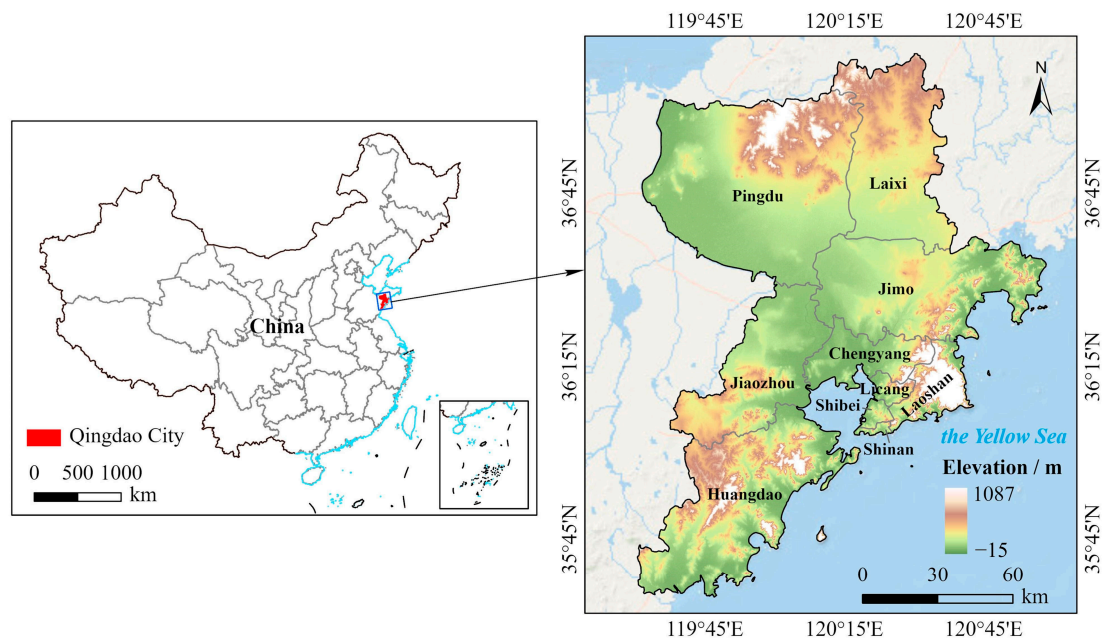


Figure 1. Location of the study area.

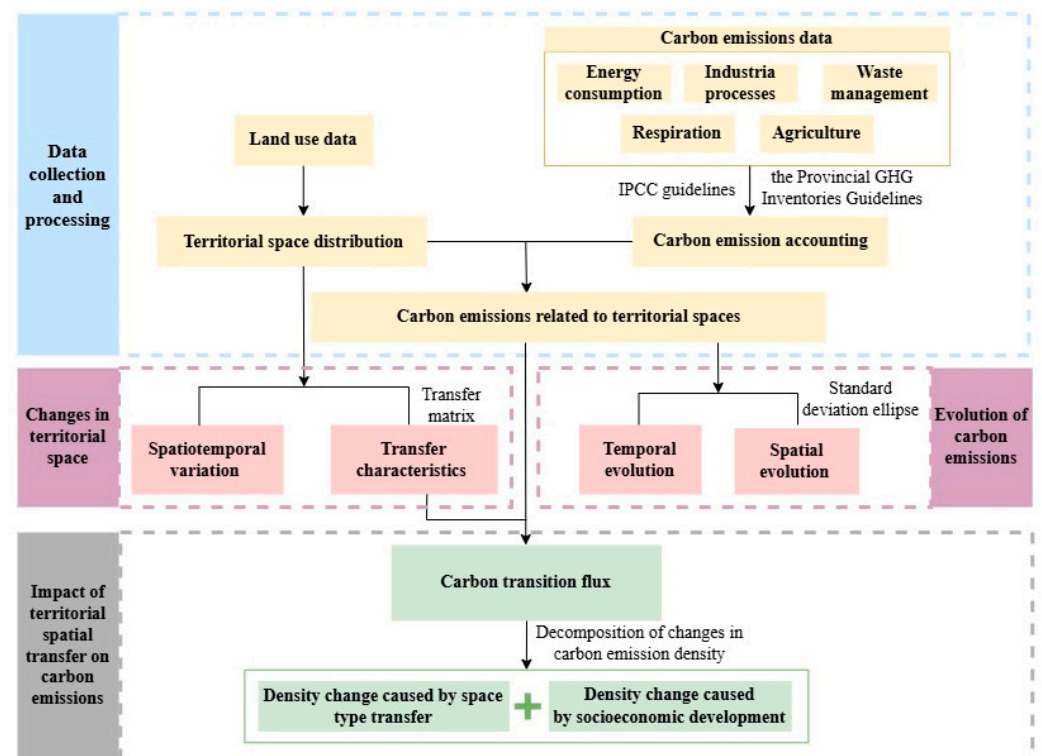


Figure 2. Technology roadmap.



### 2.2.1. Territorial Space Classification and Its Associated Carbon Emission Sectors

According to China's territorial space governance system, territorial space is regarded as an organic whole, composed of urban, agricultural, and ecological space [36]. Here, we further divide territorial space into eight distinct types based on functional differences, namely urban living space (ULS), urban production space (UPS), rural living space (RLS), agricultural production space (APS), forestland/grassland/water ecological space (FES, GES, WES), and other ecological space (OES). The classification of urban-agricultural-ecological space serves as a land use functional division scheme that correlates with various land use types [7]. Each type of space is aligned with its respective land use types so that the spatial distribution of territorial space can be obtained based on the land use/cover data.

Referring to the IPCC National Greenhouse Gas Inventories Guidelines, as well as the Provincial Greenhouse Gas Inventories Guidelines and previous studies [37–39], the primary sources of carbon emissions encompass energy consumption, industrial processes, waste management, respiration, and agriculture. Carbon sequestration predominantly occurs within terrestrial ecosystems, specifically in forests, grasslands, and wetlands. In light of the land use characteristics associated with various carbon emission activities, the refined sectors of carbon emission and carbon sequestration were systematically allocated to eight distinct territorial spaces, thus establishing a bearing relationship (Table 1). Given that the carbon emission and sequestration functions of OES are extremely weak, this space is excluded from the scope of this study.

**Table 1.** Connection between the classification of territorial space and the classification of land use and accounting catalog of carbon emissions/sinks.

Territorial Space Classification		Land Use Classification *	Catalog of Carbon Emissions/Sequestration	
Primary Space Type	Secondary Space Type	Land Use Type	Carbon Emissions	Carbon Sinks
Urban space	Urban living space (ULS)	Urban land	Energy consumption from urban households, wholesale retail trade and catering services; Urban domestic sewage; Urban domestic solid waste; Respiration of urban population.	
	Urban production space (UPS)	Other built-up land	Energy consumption from industry, construction, transport, storage, and postal services; Industrial sewage; Industrial production processes.	
Agricultural space	Agricultural production space (APS)	Paddy field, dry farmland	Energy consumption from agriculture; Rice cultivation; Agricultural production processes.	
	Rural living space (RLS)	Rural residential land	Energy consumption from rural households and graziers; Rural domestic sewage; Rural domestic solid waste; Respiration of rural population and livestock; Enteric fermentation and livestock manure.	
Ecological space	Forestland ecological space (FES)	Forestland	—	Forestland carbon uptake
	Grassland ecological space (GES)	Grassland	—	Grassland carbon uptake
	Water ecological space (WES)	Water area	—	Water carbon uptake
	Other ecological space (OES)	Unused land	—	—

\* Land Use Classification System of the Chinese Academy of Sciences.

### 2.2.2. Carbon Emission/Sequestration Calculation

Table 1 presents the carbon emission and sink accounting framework utilized in this study, which encompasses five carbon emission sectors (20 emission sub-sectors) and three carbon sink sectors. The calculations for carbon emissions and sequestration were conducted in accordance with IPCC guidelines, the Provincial GHG Inventories Guidelines, and previous studies. A comprehensive description of the calculation methodology and the parameters employed is provided in the Supplementary Materials.

Given that data pertaining to energy terminal consumption, solid waste management, and industrial sewage treatment are only accessible at the provincial level, the carbon emissions associated with these activities were determined by first calculating the emissions for Shandong Province and subsequently adjusting these figures based on the output value share or population share of the relevant sectors (e.g., industry, construction, and transportation) within Qingdao. Furthermore, the carbon emissions resulting from energy consumption and solid waste generated by urban and rural residents were estimated by apportioning the total emissions for Qingdao City in accordance with the ratio of the urban and rural permanent populations. Energy consumption from fisheries and forestry was not considered in this study.

It is important to note that, due to data constraints, this study's analysis of carbon sequestration and emissions is limited to carbon dioxide (CO<sub>2</sub>) and methane (CH<sub>4</sub>), rather than encompassing all greenhouse gases. To ensure consistency in the analysis, all results are expressed in terms of carbon. Ultimately, the carbon emissions from all sub-sectors are allocated to various territorial spaces based on the actual distribution of activities, as detailed in Table 1.

### 2.2.3. Transfer Matrix of Territorial Space

The transfer matrix denotes the configuration of the transfer area associated with alterations in territorial space, represented in a matrix format. This framework facilitates the analysis of transfer patterns and directional movements among various types of territorial spaces [16,40]

$$A_{ij} = \begin{bmatrix} A_{11} & A_{12} & \dots & A_{1n} \\ A_{21} & A_{22} & \dots & A_{2n} \\ \dots & \dots & \dots & \dots \\ A_{n1} & A_{n2} & \dots & A_{nn} \end{bmatrix} \quad (1)$$

where A denotes the area of the region. i and j represent the territorial space use type at the beginning and end of the research period, respectively. n denotes the number of territorial utilization types.

### 2.2.4. Standard Deviation Ellipse

The Standard Deviation Ellipse (SDE) is a classic method of measuring the distribution characteristics of geographic elements and their spatial-temporal evolution [41]. Taking the gravity center, the lengths of the long and short axes, azimuth, and the area of the spatial distribution ellipse as the main parameters, the SDE technique quantitatively elucidates the directionality, dispersal, and distribution patterns of the spatial distribution of geographic elements from a global spatial perspective. The gravity centers and their changing trajectories represent the relative positions of geographically dispersed elements and the directions of their spatial development. The long half-axis and short half-axis signify the direction and extent of distribution, respectively. The azimuth angle reflects the predominant distribution direction of an element. The variation in the area of the SDE provides insights into the trends of spatial contraction or expansion of these elements [42]. The SDE analysis was performed using ArcGIS 10.6, according to the calculation formulas in reference [43].

### 2.2.5. Carbon Transition Flux

The carbon transition flux is the amount of potential carbon that flows from one component of the system to another, and results in a change in the carbon stocks per unit

time and per unit area for each component [31]. In the context of urban space systems, it refers to the potential carbon flow caused by the conversion process of territorial spaces with different carbon emission/sequestration densities (i.e., carbon emissions/sequestration per unit time and per unit area). The change in carbon emission density is expressed as a carbon transition rate. The accounting for carbon transitions is conducted based on the carbon transition rate ( $\Delta D$ ) and the space area undergoing conversion ( $\Delta S$ ) between different territorial space types using the following steps.

Initially, the carbon transition rate ( $\Delta D$ ) can be calculated as follows:

$$\Delta D_{ij} = D_j - D_i = \frac{C_j}{S_j} - \frac{C_i}{S_i} \quad (2)$$

where  $i$  and  $j$  represent the initial and final types of territorial space involved in the transfer process, respectively.  $D$  represents the carbon emission density.  $C$  represents the net carbon emission associated with a specific type of space (if it is a carbon source,  $C$  is larger than 0, and if it is a carbon sink,  $C$  is less than 0).  $S$  represents the area of territorial space. If  $\Delta D < 0$ , it represents a decrease in carbon emissions or an increase in carbon sequestration, and therefore the process is beneficial; if  $\Delta D > 0$ , it represents an increase in carbon emissions or a decrease in carbon sequestration, and therefore the process is harmful.

Subsequently, carbon transition flux ( $f_{ij}$ ) between two territorial spaces is determined by multiplying the area transferred between the two types of spaces ( $\Delta S$ ) by the corresponding carbon transition rate ( $\Delta D$ ).

$$f_{ij} = \Delta D_{ij} \times \Delta S_{ij} \quad (3)$$

where  $f_{ij}$ ,  $\Delta D_{ij}$ , and  $\Delta S_{ij}$  denote the carbon transition flux, transition rate, and the transition area, respectively, associated with the transfer from space  $i$  to space  $j$ .  $\Delta S$  can be derived by computing the transfer matrix, as outlined in Section 2.2.3.

#### 2.2.6. Decomposition of Changes in Carbon Emission Density

The carbon emission density within a given territorial space is subject to variation over time due to shifts in socio-economic factors, including economic scale, technological advancement, land and environmental protection policies, and population distribution. Therefore, the changes in carbon emission density ( $T$ ) caused by the process of territorial space transition not only include the apparent density change caused by the space type transfer ( $S$ ) but also contain the underlying density changes induced by socio-economic development ( $E$ ). In this context, we reformulate the equation for the carbon transition rate to facilitate the decomposition and quantification of the density changes associated with both space type alterations and socio-economic development.

$$\Delta DT_{ij}(t_0, t) = D_j(t) - D_i(t_0) = (D_j(t) - D_j(t_0)) + (D_j(t_0) - D_i(t_0)) = \Delta DE_j(t_0, t) + \Delta DS_{ij}(t_0) \quad (4)$$

$$\Delta DE_j(t_0, t) = D_j(t) - D_j(t_0) \quad (5)$$

$$\Delta DS_{ij}(t_0) = D_j(t_0) - D_i(t_0) \quad (6)$$

where  $i$  and  $j$  represent the types of territorial space at the beginning ( $t_0$ ) and end ( $t$ ) of the research period.  $D$  represents the carbon emission density.  $\Delta DT_{ij}(t_0, t)$  is the total change in  $D$  caused by the transition from space  $i$  to space  $j$ .  $\Delta DE_j(t_0, t)$  is the density difference of space  $j$  at the end and the beginning of the period, which is influenced by socio-economic development.  $DS_{ij}(t_0)$  is the density difference between space  $j$  and space  $i$  in the initial period, that is, the difference is solely a result of the alteration in space type while maintaining the same socio-economic conditions.

#### 2.3. Data Sources

The dataset utilized in this research comprises two primary components: (1) Land-use data. The land use data for the years 2000, 2005, 2010, 2015, and 2020 were sourced from

the Data Center for Resources and Environmental Sciences of the Chinese Academy of Sciences (<https://www.resdc.cn/>, accessed on 20 September 2023). This dataset consists of 30 m Landsat TM image interpretation data, which have been categorized into six major classifications and 24 sub-classifications. For analytical purposes, these classifications have been restructured into eight distinct types of territorial space, as detailed in Section 2.2.1. (2) Socio-economic data. Statistics on energy consumption, industrial processes, waste discharge and treatment, agricultural activities, and livestock breeding for designated years were sourced from the China Energy Statistics Yearbook, the Qingdao Statistical Yearbook, the China Urban Construction Statistical Yearbook, and the China Statistical Yearbook on Environment.

### 3. Results and Analysis

#### 3.1. Spatial-Temporal Evolution Characteristics of Territorial Spaces

##### 3.1.1. Spatiotemporal Variation Characteristics

The spatial distribution of territorial spaces and the changes in the area of each space in Qingdao from 2000 to 2020 are illustrated in Figure 3. Obviously, agricultural production space (APS) was the dominant space type, accounting for approximately 65% of the total area, showing a slight fluctuation and downward trend. The area of rural living space (RLS) exhibited a continuous increase, rising from 912.28 km<sup>2</sup> (8.23%) in 2000 to 1142.30 km<sup>2</sup> (10.28%) in 2020, thereby securing its position as the second largest space type since 2005. Urban living space (ULS) experienced remarkable growth throughout the study period, with its area increasing by 1.23 times. The ULS is primarily situated around Jiaozhou Bay, and the central built-up areas of each district have expanded significantly. Conversely, urban production space (UPS) maintained the smallest proportion during the study period, initially declining by 89.98 km<sup>2</sup> between 2005 and 2010, followed by an increase of 51.17 km<sup>2</sup> in the subsequent decade. Its substantial decrease observed during 2005–2010 was mainly due to the conversion of UPS into WES in the coastal regions to the east of the Jimo district and northeast of Jiaozhou Bay.

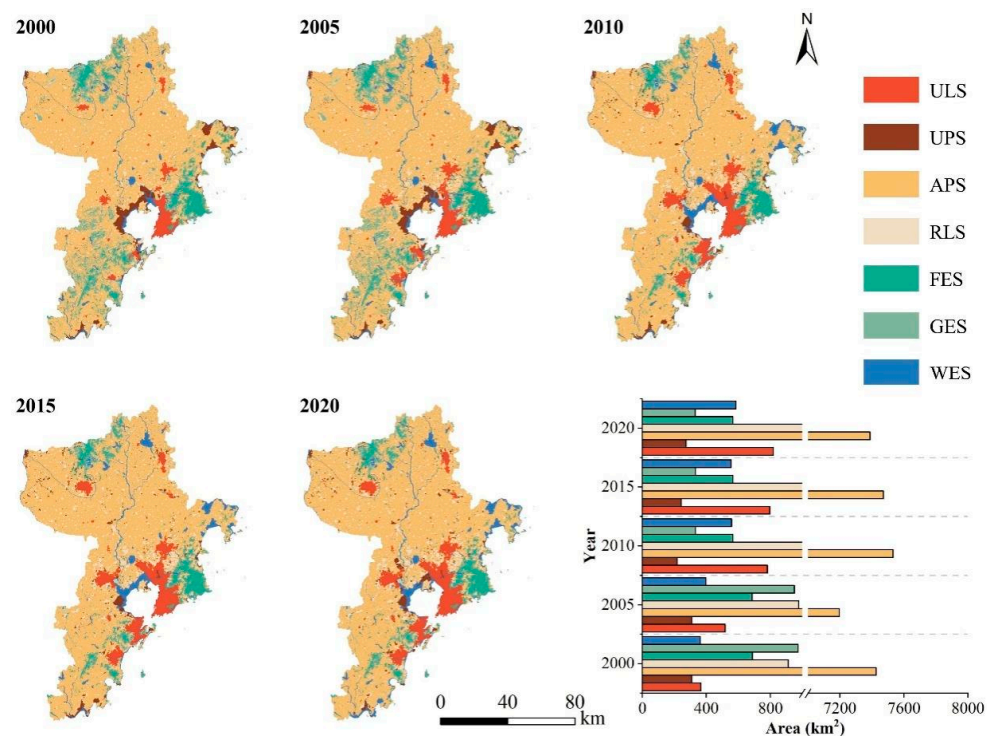


Figure 3. Spatiotemporal variation of territorial spaces in Qingdao from 2000 to 2020.



Among the ecological spaces, both grassland space and forestland space have continued to decline, with reductions of 642.45 km<sup>2</sup> and 122.13 km<sup>2</sup>, respectively. The primary regions affected by this decrease are situated in the northern Pingdu District and the southern Huangdao District. On the contrary, the area of WES has exhibited a positive trend, reflecting a total increase of 222.02 km<sup>2</sup>.

### 3.1.2. Transfer Characteristics of Territorial Space

Based on the territorial space transfer matrix, the Sankey diagram is used to show the transfer trajectory and patterns of territorial space within Qingdao city during the study period (Figure 4). Overall, approximately 22.50% of the total area experienced space transformation from 2000 to 2020. Notably, there was a frequent outflow and inflow of APS and RLS, alongside the outflow of GES and the inflow of ULS. Among them, the most converted type is from GES to APS (538.75 km<sup>2</sup>), accounting for 55.35% of the total GES area. APS underwent the most substantial alterations, with 993.36 km<sup>2</sup> exiting and 953.58 km<sup>2</sup> entering. Most of the converted APS was repurposed into RLS (45.24%), ULS (28.63%), and UPS (13.70%). ULS exhibited a net increase of 445.14 km<sup>2</sup>, primarily resulting from transformations from APS (284.38 km<sup>2</sup>) and RLS (78.58 km<sup>2</sup>). The net increase in RLS was dominated by the reciprocal conversions between APS and RLS. Additionally, 121.24 km<sup>2</sup> of FES was converted into APS, constituting 77.43% of the total FES transformations. The transfer trajectory from UPS to WES determined the net decrease of UPS (41.11 km<sup>2</sup>) and the net increase of WES (191.78 km<sup>2</sup>).

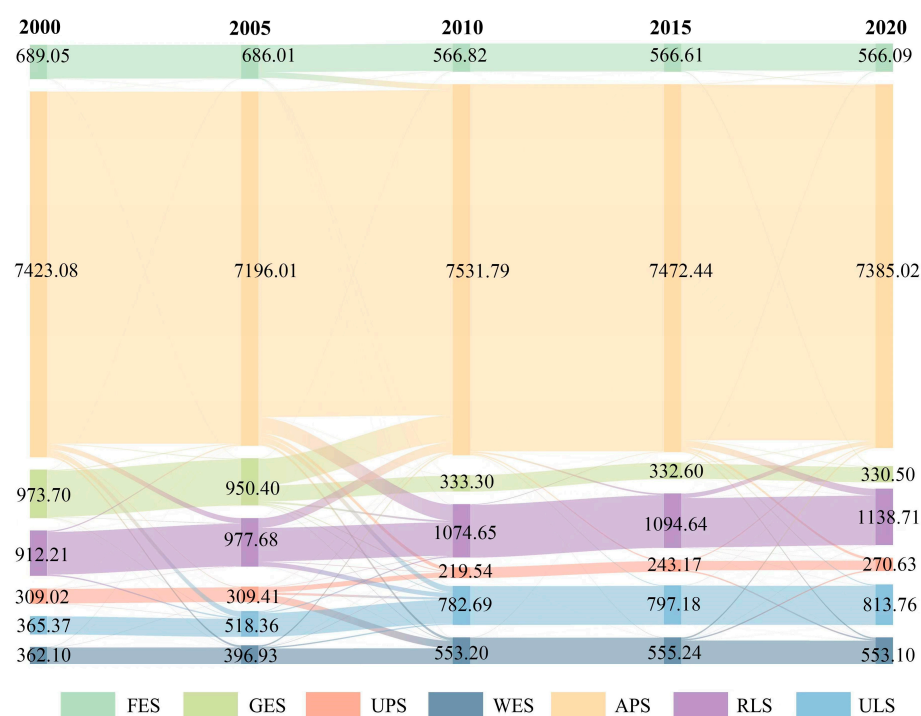


**Figure 4.** The trajectory of territorial space transfers in Qingdao city from 2000 to 2020.

From the viewpoint of the transition period, the most significant change occurred between 2005 and 2010, when Qingdao city underwent a transformation in 18.12% of its total area. In contrast, the conversion areas in the other three periods were much smaller, with only 3.84% from 2000–2005, 1.02% from 2010–2015, and 4.88% from 2015 to 2020. The substantial shift from GES to APS during 2005–2010 led to the only increase in APS area (335.64 km<sup>2</sup>) during that time. Over the span of two decades, Qingdao's primary transformation trend was from agricultural and ecological spaces to residential areas, highlighting the significant impact of socio-economic development and human activities on land resources.

### 3.2. Spatiotemporal Evolution Characteristics of Carbon Emissions in Territorial Spaces

#### 3.2.1. Temporal Changes in Carbon Emissions

Figure 5 depicts the changing trends of total carbon emissions/sequestration across seven territorial spaces from 2000 to 2020. In general, carbon emissions in Qingdao showed an increasing trend, with the total net carbon emissions increasing from  $313.98 \times 10^4$  tons to  $1068.58 \times 10^4$  tons. Among the four carbon source spaces, UPS recorded the highest emissions, which rose from  $185.08 \times 10^4$  tons (57.94% of total emissions) in 2000 to  $751.04 \times 10^4$  tons (69.96%) in 2020. ULS experienced the most significant growth in emissions, surging 9.60 times over the two decades to reach  $192.69 \times 10^4$  tons by 2020. In contrast, RLS had the slowest growth rate, with emissions increasing by 17% from  $102.96 \times 10^4$  tons in 2000 to  $120.61 \times 10^4$  tons in 2020. Only APS exhibited a decline in carbon emissions, falling from  $13.23 \times 10^4$  tons to  $9.25 \times 10^4$  tons.

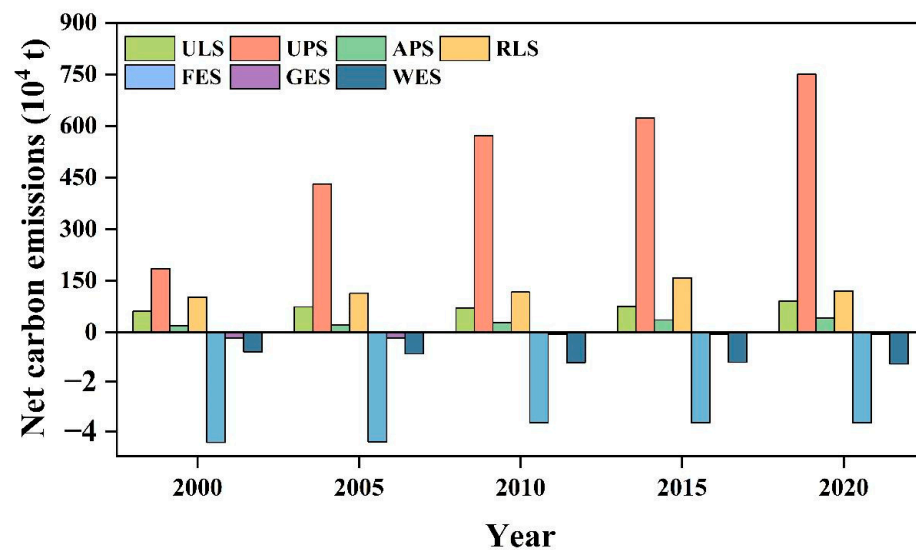


**Figure 5.** Temporal variation of carbon emission in territorial spaces.

In comparison, the change in carbon sequestration is quite minor. FES plays a larger role in the overall carbon sink. Due to the area reduction of FES and GES, the carbon sinks in both spaces have significantly declined, dropping from  $4.43 \times 10^4$  tons and  $0.23 \times 10^4$  tons to  $3.65 \times 10^4$  t and  $0.08 \times 10^4$  tons, respectively. On a positive note, the carbon sequestration capacity of WES has been greatly improved, growing from  $0.79 \times 10^4$  tons in 2000 to  $1.27 \times 10^4$  tons in 2020.

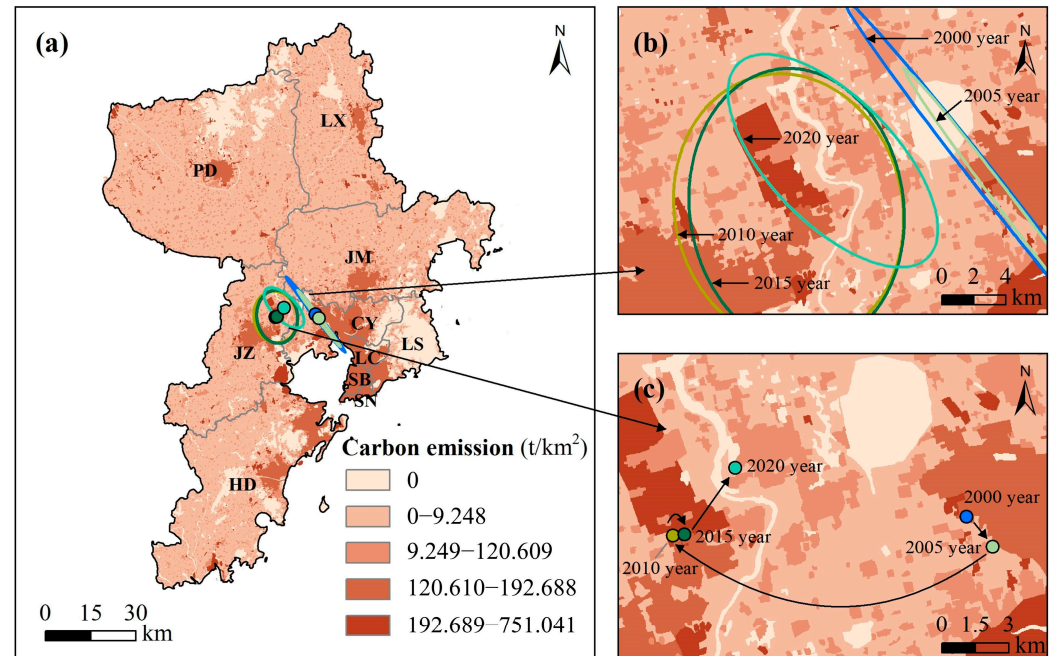
In terms of carbon emission density (Table 2), UPS exhibits a significantly higher emission density compared to other spaces, primarily due to its substantial energy consumption and industrial activities. In these 20 years, the emission density of UPS has nearly tripled, soaring from  $5988.98 \text{ t/km}^2$  in 2000 to  $30,879.02 \text{ t/km}^2$  in 2015, followed by a slight decrease. The carbon emission density of RLS exhibited a fluctuating downward trend from  $1128.57 \text{ t/km}^2$  in 2000 to  $1055.84 \text{ t/km}^2$  in 2020, and its ranking fell from second place before 2010 to third place after 2015. In contrast, the emission density of ULS has risen significantly, reaching 4.72 times its 2000 level, making it the second most intense space after 2015. Recently, the growing urban population and enhanced living standards have exacerbated household energy consumption and waste production, which have contributed to the rise in carbon emission density. APS recorded the lowest carbon emission density, which has fluctuated downwards from  $17.82 \text{ t/km}^2$  in 2000 to  $12.52 \text{ t/km}^2$  in 2020. FES, GES, and WES serve as vital carbon sink spaces, maintaining stable carbon emission densities at approximately  $-64.40 \text{ t/km}^2$ ,  $-2.40 \text{ t/km}^2$ , and  $-21.80 \text{ t/km}^2$ , respectively.

**Table 2.** Carbon emission density of different territorial spaces in Qingdao ( $t\ C/km^2$ ).

Type	2000	2005	2010	2015	2020
ULS	497.38	643.27	908.58	2416.86	2351.46
UPS	5988.98	13,960.04	26,026.22	30,879.02	27,442.29
APS	17.82	19.33	15.28	12.38	12.52
RLS	1128.57	1169.86	1091.4	1101.78	1055.84
FES	−64.40	−64.40	−64.40	−64.40	−64.40
GES	−2.40	−2.40	−2.40	−2.40	−2.40
WES	−21.80	−21.80	−21.80	−22.80	−21.80

### 3.2.2. Spatial Distribution and Evolution Characteristics of Carbon Emissions

Table 3 and Figure 6 present the parameters and distribution of the standard deviational ellipse (SDE) pertaining to carbon emissions for each year. The data indicate that the carbon emissions of Qingdao City form a relatively stable “northwest–southeast” distribution pattern. Throughout the observed period, the area of the SDE demonstrated a fluctuating upward trend, increasing from  $35.79\ km^2$  to  $106.09\ km^2$ , which signifies an expansion in the spatial dispersion of carbon emissions. Analyzing the long half-axis reveals a significant reduction from  $15.86\ km$  to  $8.57\ km$  between 2000 and 2010, followed by a period of stability until 2020. This trend suggests a centripetal agglomeration of carbon emissions in the northwest–southeast direction. Compared with other regions, the main urban area experienced accelerated economic growth and a higher degree of population concentration from 2000 to 2010, leading to larger and more concentrated carbon emissions. On the contrary, there was a notable increase in the short half-axis, indicating a decrease in the oblateness of the SDE, which reflects an increase in the dispersion of carbon emissions and a weakening of directional tendencies.

**Figure 6.** The directional distribution and gravity center of carbon emissions from 2000 to 2020 (a) with a standard deviational ellipse change pattern (b) and gravity center migration paths (c).

As for the moving track of the gravity center, the gravity center of carbon emissions in Qingdao City has cumulatively shifted  $20.40\ km$  to the northwest on the whole. The two major migrations were the westward shift ( $14.35\ km$ ) during 2005–2010 and the northeastward movement ( $3.76\ km$ ) from 2015 to 2020. This phenomenon is likely attributable to the economic development of the northwestern counties of Jiaozhou, Pingdu, and Laixi, which

has led to an increase in local carbon emissions, thereby influencing the relocation of the emission center in that direction.

**Table 3.** The parameters of the carbon emission standard deviation ellipse and gravity center in Qingdao from 2000 to 2020.

Year	Area /km <sup>2</sup>	Long Half-Axis /km	Short Half-Axis /km	Azimuth/°	The Coordinates of the Gravity Center
2000	35.79	15.86	0.72	141.82	120.25° E, 35.65° N
2005	19.20	11.78	0.52	142.80	120.26° E, 35.64° N
2010	192.82	8.57	7.16	167.50	120.11° E, 35.66° N
2015	186.60	8.83	6.73	172.31	120.11° E, 35.66° N
2020	106.09	8.53	3.96	135.66	120.14° E, 35.68° N

Consistent with carbon emissions, carbon sinks in Qingdao city also exhibited a “northwest–southeast” distribution pattern, with the azimuth angle initially shifting towards the north and subsequently towards the west (Table 4 and Figure 7). The SDE area experienced a notable reduction, measuring only 0.75 km<sup>2</sup> in 2020, which indicates a significant contraction in the distribution of carbon sinks. Furthermore, the average length (8.54 km) and the length variation (1.73 km) of the long half-axis of the carbon sink SDE were considerably less than those associated with carbon emissions, suggesting a more stable and distinctly centripetal distribution of carbon sinks. The substantial reduction in the short half-axis contributes to an increase in elliptic oblateness, thereby reflecting an enhancement in the centrality and directional orientation of carbon sinks.

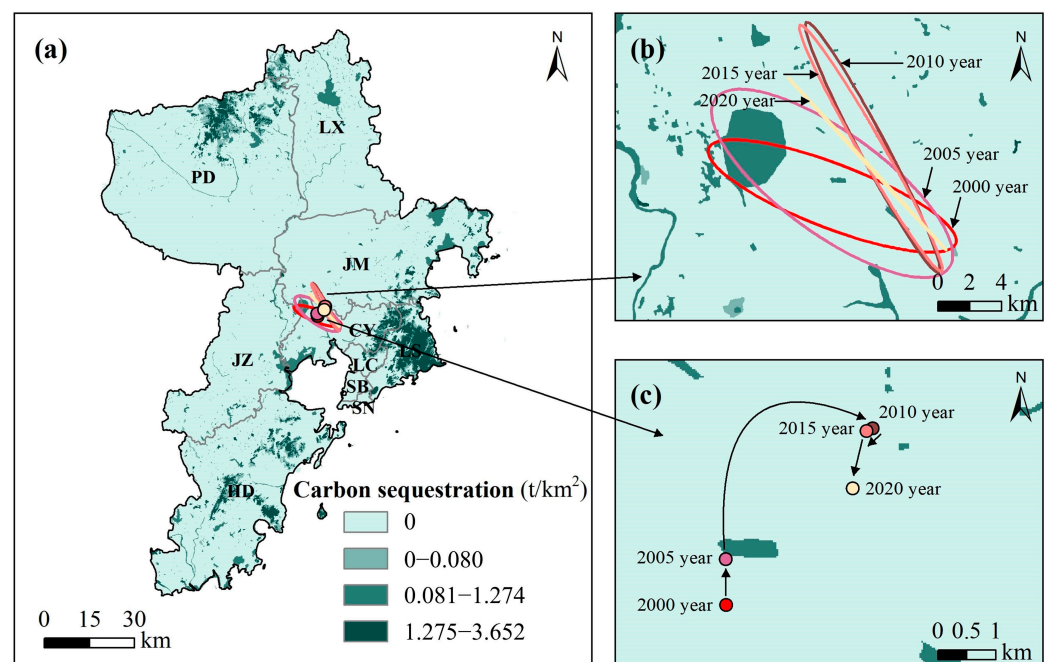


**Figure 7.** The directional distribution and gravity center of carbon sinks from 2000 to 2020 (a) with a standard deviational ellipse change pattern (b) and gravity center migration paths (c).

The gravity center displayed an overall migration of 5.35 km to the northeast from 2000 to 2020. Likewise, substantial migration events were observed during the intervals of 2005–2010 and 2015–2020, during which the center of gravity shifted 3.42 km to the northeast and 1.02 km to the southwest, respectively.



**Table 4.** The parameters of the carbon sink standard deviation ellipse and gravity center in Qingdao from 2000 to 2020.

Year	Area /km <sup>2</sup>	Long Half-Axis /km	Short Half-Axis /km	Azimuth/°	The Coordinates of the Gravity Center
2000	52.87	8.35	2.01	111.03	120.27° E, 35.67° N
2005	91.74	9.09	3.21	125.81	120.27° E, 35.67° N
2010	23.86	8.92	0.85	152.00	120.30° E, 35.69° N
2015	21.20	8.96	0.76	150.01	120.30° E, 35.69° N
2020	0.75	7.36	0.04	137.46	120.29° E, 35.68° N

3.3. Impact of Territorial Spatial Transfer on Carbon Emissions

3.3.1. Carbon Transition Flux Caused by Space Transfers

Utilizing the transfer matrix of territorial space alongside the carbon transition rate, the carbon transition flux resulting from space transfers was computed for each designated period. The net carbon transition fluxes during the four periods (2000–2005, 2005–2010, 2010–2015, and 2015–2020) were  $30.96 \times 10^4$  tons,  $37.19 \times 10^4$  tons,  $80.24 \times 10^4$  tons, and  $65.64 \times 10^4$  tons, respectively. These positive net fluxes suggest that harmful carbon transition fluxes significantly outweighed the beneficial ones, implying that the transfer of territorial space in the four periods all exerted detrimental effects on the carbon emissions in Qingdao City. Table 5 delineates the primary beneficial and harmful space transfer paths, along with the corresponding carbon transfer flux and their respective contribution rates.

**Table 5.** Main space transfer paths, fluxes, and contribution rates of major beneficial and harmful carbon transitions in Qingdao city.

Years	Beneficial Carbon Transition			Harmful Carbon Transition		
	Main Space Transfer Path	Carbon Transition Flux (×10 <sup>3</sup> t)	Contribution Rate %	Main Space Transfer Path	Carbon Transition Flux (×10 <sup>3</sup> t)	Contribution Rate %
2000–2005	UPS → ULS	−34.01	25.45	APS → UPS	149.25	33.67
	RLS → APS	−27.17	20.33	APS → RLS	120.78	27.25
	UPS → RLS	−26.44	19.79	APS → ULS	68.94	15.55
	UPS → APS	−19.52	14.61	WES → UPS	55.31	12.48
	RLS → ULS	−13.06	9.77	GES → UPS	23.89	5.39
	—	—	—	GES → RLS	9.04	2.04
2005–2010	UPS → WES	−2085.01	66.41	APS → UPS	1950.95	55.56
	UPS → ULS	−601.85	19.17	GES → UPS	443.1	12.62
	RLS → APS	−223.74	7.13	APS → RLS	346.54	9.87
	UPS → RLS	−105.72	3.37	RLS → UPS	236.73	6.74
	UPS → APS	−69.78	2.22	WES → UPS	185.51	5.28
	—	—	—	APS → ULS	104.29	2.97
2010–2015	UPS → WES	−38.03	39.60	APS → UPS	798.99	88.93
	UPS → APS	−35.49	36.96	APS → ULS	35.54	3.96
	RLS → APS	−13.14	13.68	APS → RLS	34.63	3.85
	UPS → GES	−2.3	2.40	WES → UPS	9.62	1.07
	UPS → RLS	−1.97	2.05	—	—	—
2015–2020	UPS → WES	−897.31	49.56	APS → UPS	1375.33	55.75
	UPS → APS	−676.66	37.37	WES → UPS	746.31	30.25
	RLS → APS	−96.17	5.31	APS → RLS	139.88	5.67
	UPS → RLS	−54.97	3.04	RLS → UPS	65.52	2.66
	UPS → FES	−23.03	1.27	APS → ULS	48.08	1.95
	—	—	—	GES → UPS	36.73	1.49

The transfer of urban production space to other types of space is the main contributor to beneficial carbon transitions, with their total contribution rates reaching 65.83%, 91.41%,

84.06%, and 93.11% in the four periods, respectively. Among them, the path with the largest contribution during 2000–2005 was “UPS to ULS” (25.45%); in the subsequent three periods, the predominant transitions were all “UPS to WES” (66.41%, 39.60%, and 46.56%, respectively). In addition, the transfer of RLS to APS emerged as another critical beneficial transfer pathway, resulting in carbon fluxes of  $-27.17 \times 10^3$  tons,  $-223.74 \times 10^3$  tons,  $-13.14 \times 10^3$  tons, and  $-96.17 \times 10^3$  tons across the four periods, respectively. Regarding the harmful carbon transition, the outflow from APS to the other three carbon source spaces—UPS, RLS, and ULS—was the most significant contributor, accounting for 76.47%, 68.40%, 96.74%, and 63.37% of the harmful carbon fluxes in the four periods, respectively. Additionally, the transfers of Waste Energy Space (WES) and Green Energy Space (GES) to UPS were also notable harmful transfer pathways across all four periods.

### 3.3.2. Changes in Carbon Emission Density Caused by Space Type Transfer and Socio-Economic Development

The spatial distribution of changes in carbon emission density (DTC) caused by the process of territorial space conversion is shown in Figure 8a. The DTC for each period is decomposed into two components, namely the explicit density changes attributable to modifications in space type (DSC, Figure 8b) and the implicit density changes associated with variations in socio-economic level (DEC, Figure 8c).

From 2000 to 2005, a notable positive density difference was observed across most regions, primarily attributed to the increase in DEC within four designated carbon source areas. The distribution of DSC is relatively sporadic, with a concentration in proximity to urban space. Among them, the positive density difference was predominantly linked to the transition from APS to ULS (yellow patches,  $479.57 \text{ t/km}^2$ ) and from APS to RLS (orange patches,  $1110.76 \text{ t/km}^2$ ). Conversely, beneficial transitions, particularly from APS to WES in the northern regions (green patches,  $-39.60 \text{ t/km}^2$ ), as well as from RLS to ULS and APS around urban space (blue patches,  $-631.19 \text{ t/km}^2$  and  $-1110.75 \text{ t/km}^2$ , respectively), contributed to a reduction in density within these areas (Figure 8(b2)).

The carbon emission density in Qingdao City experienced the most drastic territorial space transformation during 2005–2010. The concentration of urban population and industrial development led to an increase in DEC from ULS and UPS by  $265.31 \text{ t/km}^2$  (yellow patches) and  $12,066.18 \text{ t/km}^2$  (orange patches), respectively. On the contrary, the DEC of APS and RLS decreased by  $4.05 \text{ t/km}^2$  and  $78.46 \text{ t/km}^2$ , respectively (green patches, Figure 8(c2)). This substantial space transformation resulted in a spatially heterogeneous distribution of DSC across approximately 18% of the area, of which the transition of ecological spaces (FES, GES, and WES) to APS resulted in a density increase of less than  $100 \text{ t/km}^2$  in about 42% of the conversion area. The pronounced increase of DSC ( $>10,000 \text{ t/km}^2$ ) was primarily attributed to the conversion of other spaces to UPS. Beneficial DSC occurred over a large area near Jiaozhou Bay and in the eastern coastal regions of Jimo District, with the most significant contributions arising from the conversion of UPS to WES and ULS (blue patches, Figure 8(b2)).

In contrast, the proportion of regions exhibiting a transition in space type from 2010 to 2020 is minimal, indicating that approximately 99% of the observed changes in DTC are attributable to DEC. With the exception of APS, the emission density of the other three carbon source spaces increased to varying degrees (Table 2 and Figure 8(c3)). However, this situation was reversed in the last period. Only the emission density (DEC) of APS increased slightly ( $0.14 \text{ t/km}^2$ ), while the DEC of the other three carbon source spaces decreased by  $65.40 \text{ t/km}^2$  (ULS),  $3436.72 \text{ t/km}^2$  (UPS), and  $45.94 \text{ t/km}^2$  (RLS), respectively (Figure 8(c4)). The pronounced and concentrated areas of DSC in the northwestern region of Jiaozhou can be attributed to the conversion from APS to UPS, which resulted in a substantial density increase of  $30,866.64 \text{ t/km}^2$  (Figure 8(b4)). In addition, the interconversion between RLS and APS played a pivotal role in driving both beneficial and harmful changes in DSC, respectively.

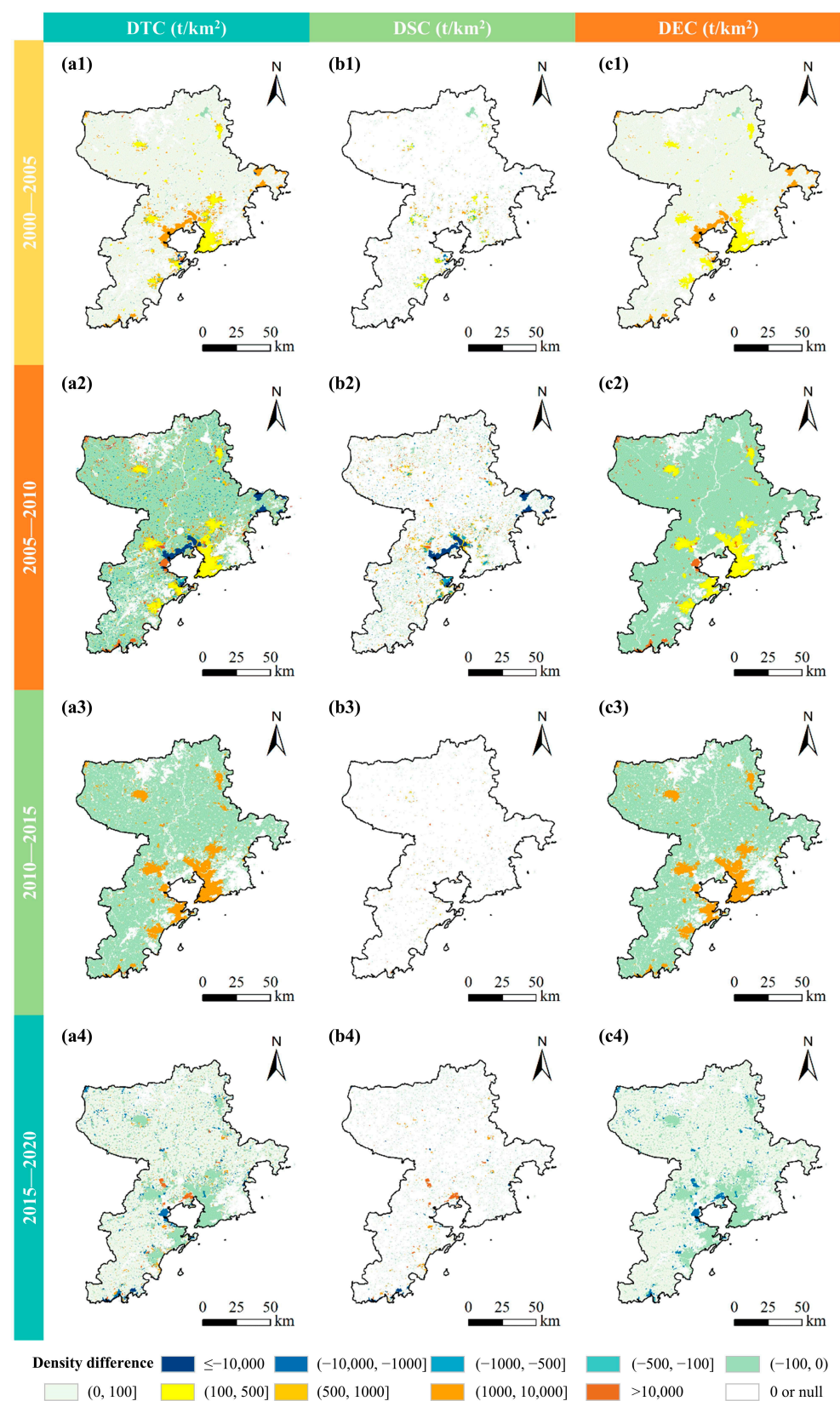


**Figure 8.** The distribution of total changes in carbon emission density (DTC), density change caused by space type transfer (DSC), and density change caused by socio-economic development (DEC) in Qingdao City from 2000 to 2020. (a–c) represent DTC, DSC, and DEC, respectively; 1, 2, 3, and 4 correspond to the four distinct time intervals: 2000 to 2005, 2005 to 2010, 2010 to 2015, and 2015 to 2020.

## 4. Discussion

### 4.1. Evolution of Territorial Spaces and Its Effect on Carbon Emissions

Generally, the transformation of the territorial space structure in Qingdao between 2000 and 2020 is mainly characterized by an expansion of residential space and a contraction of both production and ecological spaces, which is in line with the findings of the investigation of Jia and Yin [44]. Qingdao is a fast-growing city with a continuous influx of people, whose urbanization rate grew to the highest in the province by 2017 and reached as high as 76.34% in 2020 [45]. To accommodate the growing population, ULS and RLS expanded by 122.73% and 24.87%, respectively, in these 20 years. Spatially, influenced by planning initiatives such as “One Valley, Two Districts” and “Three Bays and Three Cities”, Qingdao has gradually formed a municipal district pattern around Bohai Bay [46]. The Huangdao district, designated as a state-level new area, has significantly contributed to the urban development of the southwestern region of Jiaozhou Bay, thereby facilitating the expansion of ULS (Figure 3). Concurrently, inland county-level cities exhibited divergent sprawl from the county seat to the periphery. Most of the newly added living space is converted from APS, which caused an increase in carbon emissions in these areas, while the multi-directional expansion of living space has further exacerbated the spatial dispersion of carbon emissions. The study conducted by Zhang et.al [47] also corroborated that carbon emissions in urban areas in Qingdao increased significantly from 2000 to 2020, exhibiting a pattern of outward expansion. The per capita ULS in Qingdao rose from 85.30 m<sup>2</sup> in 2000 to 136.47 m<sup>2</sup> in 2010, before gradually declining to 105.48 m<sup>2</sup> by 2020, indicating an improvement in the efficiency of ULS utilization. However, the phenomenon of “decreasing rural population vs. increasing RLS” was very prominent in Qingdao, resulting in a rise in the per capita RLS from 284.16 m<sup>2</sup> in 2000 to 476.42 m<sup>2</sup> in 2020, significantly surpassing the national standard for per capita rural construction [48]. Consequently, while efforts to optimize per capita ULS continue, it is essential to intensify measures aimed at controlling and reducing RLS, as well as promoting its conversion into APS and ecological spaces, as a critical strategy for mitigating carbon emissions.

UPS was initially concentrated in coastal areas but has gradually spread inland since 2010 (Figure 3). The transformation of large-scale UPS to WES is mainly due to the conversion of salt pans into ponds or shoals. Notwithstanding a decrease in area, carbon emissions from UPS have persistently increased over the past two decades. This trend can be attributed to a heightened emission density resulting from the expansion of industrial scale and energy consumption. From the perspective of space transformation, the transfer of UPS to other spaces has significantly contributed to the beneficial carbon transitions. This indicates that carbon emissions can be mitigated through two primary strategies: first by regulating the area of UPS through enhanced intensive and economical land use practices, thereby facilitating its transition to other spaces, and second by decreasing emission intensity through advancements in production technology and improvements in energy efficiency. The widespread expropriation of APS for urban production and resident living spaces in the past 20 years has resulted in the greatest harmful carbon transition (Table 5). Therefore, controlling its transfer to other carbon source spaces is very essential for both ensuring regional food security and achieving carbon emission reduction.

### 4.2. The Evolution of Carbon Emissions in Qingdao and Its Implications

To date, there is no officially recognized and standardized methodology for measuring city-scale carbon emissions. To assess the validity of the accounting results in this paper, the emission inventories for 290 Chinese Cities from 1997 to 2019, as published by the China Emission Accounts and Datasets (CEADs) (<https://www.ceads.net.cn/>, accessed on 10 September 2023), were utilized as benchmark data for carbon emissions. By comparison, the total carbon emissions for Qingdao city calculated in this paper are approximately 0.5 times greater than those reported in the corresponding datasets for the same years. This discrepancy can be attributed primarily to the incomplete nature of the CEADs accounting, which only considers energy-related and process-related emissions from industrial activ-



ities while neglecting emissions from other sectors such as agriculture, land use change and forestry, and waste management [49]. Overall, the carbon accounting methodology employed in this study, which is grounded in actual statistical data and pertinent research (as detailed in the Supplementary Materials), is deemed to be relatively sound and credible.

In recent years, some scholars, using carbon emissions data from the ODIAC database, have revealed the continuous rise in carbon emissions in Qingdao between 2000 and 2020 and identified socio-economic development as the key driver of this increase [32,47]. However, these studies focused solely on carbon emissions from fossil fuels and did not explore the differences in the impact of space type changes and socio-economic development on carbon emissions during land use transitions. This paper proposes a carbon transition decomposition formula to quantify the differential and spatially heterogeneous impacts of changes in space types and socio-economic development on emissions. The results indicate that DEC predominantly shapes the global patterns of regional emission density alterations, whereas space transfer primarily accounts for local variations (Figure 8). This means that the biggest contribution to carbon emission growth is the increase in emission density in carbon source spaces caused by socio-economic development. Specifically, the 2.4-fold increase in Qingdao's net carbon emissions during the study period is mainly attributed to the sprawl of urban space and the surge in their emission densities (Figure 3 and Table 2). This assertion is further supported by the significant increase in the share of total carbon emissions from both UPS and ULS, which widened from 63.67% in 2000 to 91.57% in 2020 (Figure 9). From the perspective of emission structure, industrial energy consumption contributes the most to emissions in UPS (accounting for 85.2% on average), with its proportion rising in recent years. By 2020, Qingdao was still in the late middle period of industrialization as a whole and the corresponding industrialization task had not yet been completed [34]. In this context, optimizing the energy structure—specifically by increasing the share of cleaner energy sources such as natural gas—and enhancing energy efficiency through technological advancements are identified as the most effective strategies for mitigating emissions in UPS [50]. The transport, storage, and postal services (TSPS) sector ranks as the second largest contributor to emissions within UPS. The reduction of its emissions ratio in 2020 is likely due to the decreased energy intensity and repercussions of the COVID-19 pandemic. However, ongoing urbanization and industrialization are likely to escalate the demand for TSPS. Strategies such as substituting high-carbon energy sources, expanding electric vehicle infrastructure, and developing hydrogen energy are potential avenues for further emission reductions [51]. In the context of ULS, the proportion of energy consumption emissions has remained stable at around 33%. Notably, solid waste emissions surged to the forefront, accounting for 41% in 2020. This trend underscores the importance of encouraging residents to adopt low-carbon lifestyles [35], promoting the classification of solid waste, and transitioning waste disposal methods from landfilling to incineration as effective strategies for reducing emissions in ULS [33].

In contrast, the growth in total emissions from agricultural space was very slight, resulting in a substantial reduction of its share by 24.7%. The primary contributors to emissions were human and animal respiration, as well as livestock breeding; however, due to a concurrent decline in both the rural population and livestock breeding scale, their share decreased from 76.84% to 59.85%. Additionally, there was a notable rise in the emission of solid waste in RLS. Carbon emissions from APS, which account for the smallest proportion, are primarily associated with the use of fertilizers, pesticides, and plastic films. This highlights the critical role of optimizing and regulating the use of agricultural inputs to meet emission reduction targets [52].

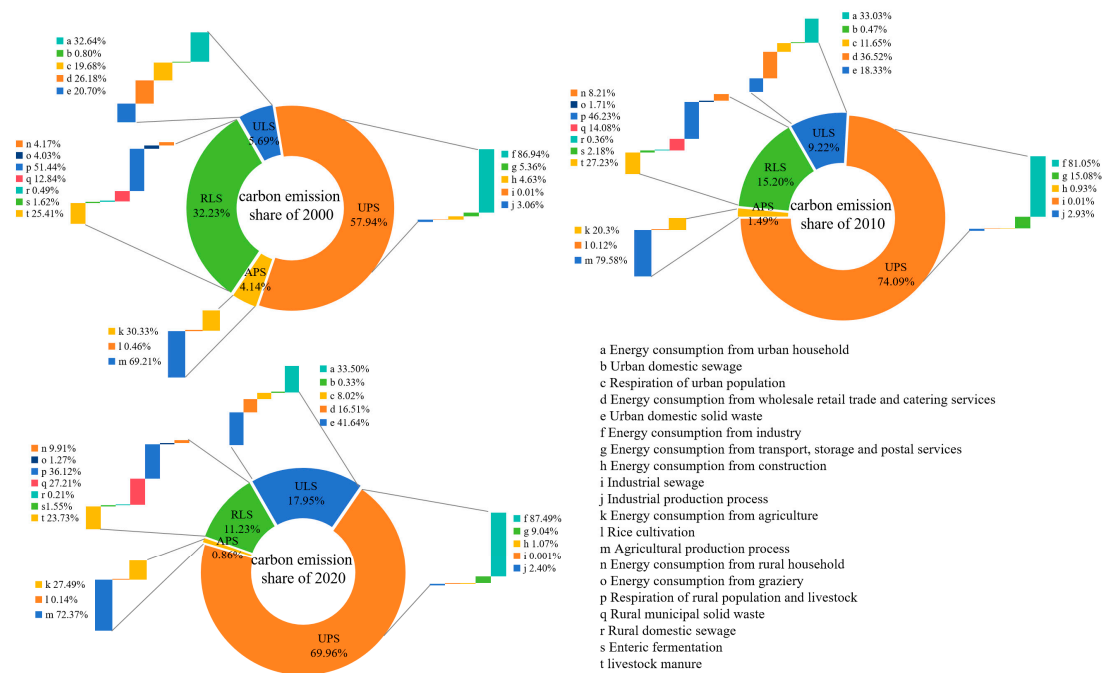


**Figure 9.** Changes in the carbon emission structure in different territorial spaces in Qingdao.

#### 4.3. Implication for Territorial Spatial Planning and Governance

The impact characteristics of territorial space evolution on carbon emissions can offer significant insights for the development or adjustment of urban spatial planning and governance strategies that aim to foster low-carbon development. The increase in net carbon emissions in Qingdao can largely be attributed to the expansion of urban space coupled with the reduction of ecological space. From a planning perspective, it is essential to scientifically delineate or adjust urban development boundaries and ecological protection red lines, while rigorously restricting the growth of urban spaces and the contraction of ecological spaces. In terms of spatial regulation, it is imperative to implement necessary measures, such as promoting three-dimensional development and increasing the minimum floor area ratio, to enhance the economical and intensive use of urban land [53,54]. Concurrently, the construction of urban green space networks and the ecological restoration of forests and grassland are crucial for augmenting ecological land. Furthermore, it is advisable to explore land use policies through the lens of low-carbon land use regulations and planning. For instance, imposing restrictions on land use for traditional high-carbon industrial projects and enacting preferential land supply policies for low-carbon industrial projects channel capital into low-carbon industries and promote the transformation of regional industrial structures into low-carbon structures [19].

At the county scale, it is possible to develop tailored land use structure adjustment plans and implement differentiated land use supply models that take into account the carbon emission profiles of various counties [55]. For Pingdu, Huangdao, and Laoshan, which have important ecological source zones, it is imperative to prioritize the preservation of the existing land use structure while promoting the development of low-carbon industries, and strict controls should be enforced regarding the extent of forest land, grassland, and water areas within these ecological sources. For the counties/districts with high carbon emissions, which are mainly situated around Bohai Bay, it is recommended that future policies for construction land use should be tightened reasonably.

To achieve more detailed insights, it is advisable to perform further multi-scenario land use predictions and micro-scale carbon balance zoning. Such efforts can aid in the adjustment and optimization of land use structures [23,55].

#### 4.4. Limitations and Future Research

This study assesses the carbon emissions associated with territorial spaces in Qingdao by utilizing a range of statistical data and adhering to the IPCC guidelines, the Provincial Greenhouse Gas Inventories Guidelines, and prior research. However, there are still the following deficiencies in the calculation process: (1) Due to constraints in data availability, the carbon emissions for certain sectors, including energy consumption, solid waste, and industrial sewage, are derived from provincial accounting results based on output or population ratios, which may result in discrepancies in the accounting. (2) The energy consumption from fisheries related to water bodies is not considered in this paper. The fishery sector in Qingdao constitutes a significant element of marine aquaculture; however, current statistical data do not distinguish between freshwater and marine fisheries. As a result, there is a lack of adequate information to accurately assess carbon emissions stemming from energy consumption related to fisheries in terrestrial water bodies. Considering the significant importance of carbon accounting, it is imperative that future research endeavors focus on enhancing foundational studies related to carbon accounting, as well as the validation of carbon accounting data at the municipal level and lower.

#### 5. Conclusions

Based on the relationship between territorial spaces and carbon emission sectors, this paper calculated the carbon emissions associated with territorial spaces in Qingdao from 2000 to 2020. It investigates the spatiotemporal dynamics of territorial spaces alongside their corresponding carbon emissions, identifies the contribution of various space transfer paths to carbon emissions, and disaggregates the differential impacts of space type changes and socio-economic development.

From 2000 to 2020, living spaces in Qingdao have significantly expanded, with ULS and RLS increasing by 122.73% and 24.87%, respectively. Conversely, both production land and ecological land experienced a decline to varying extents. The total net carbon emissions in Qingdao rose from  $313.98 \times 10^4$  tons to  $1068.58 \times 10^4$  tons, with UPS contributing the most (69.96% in 2020) due to its exceptionally high emission density. The spatial distribution of carbon emissions and carbon sinks both formed a stable “northwest–southeast” pattern. Carbon emissions are becoming increasingly dispersed spatially and exhibiting diminished directionality, while carbon sinks are demonstrating an opposing trend.

The transformation of the territorial space exerted detrimental effects on carbon emissions in Qingdao City. The transfer of UPS to other spaces has primarily facilitated positive carbon transitions, whereas the expropriation of APS for urban production and residents' living has resulted in the most significant harmful carbon transition. Socio-economic development predominantly shapes the global patterns of regional emission density alterations, whereas space transfer primarily accounts for local variations.

In light of these findings, it is advisable that the urban development boundaries and ecological protection red lines of Qingdao City should be scientifically delineated to restrict the growth of urban spaces and the contraction of ecological spaces. We recommend the implementation of incentive-based or restrictive policies aimed at fostering the economical and intensive utilization of urban land, while also imposing limitations on land designated for high-carbon industries. Furthermore, we propose the establishment of differentiated structural adjustment and land supply models that take into account the carbon emission profiles of various counties/districts. Our research may serve as a valuable reference for other cities seeking to advance low-carbon development through spatial optimization strategies. For low-carbon optimization at the local scale, future research should prioritize the development of multi-scenario land use predictions and micro-scale carbon balance zoning to inform the adjustment and optimization of land use structures. At the national and international levels, it is essential to investigate the variations in carbon balance and emission characteristics across different regions, thereby enabling the formulation of tailored low-carbon development strategies for each specific area.

**Supplementary Materials:** The following supporting information can be downloaded at: <https://www.mdpi.com/article/10.3390/land13101717/s1>, Supplementary Text: Carbon emission accounting methods; Table S1: Net calorific value of energy and carbon emission factor; Table S2: Carbon emission coefficients of the production process of major industrial products in Qingdao; Table S3: Carbon emission factors for different agricultural inputs; Table S4 Methane emission factors for animal enteric fermentation; Table S5: Methane emission factors for animal manure management. References [56–62] are cited in the supplementary materials.

**Author Contributions:** Conceptualization, B.N. and J.H.; methodology, B.N., J.H. and X.L. (Xiangfei Liu); software, J.H. and X.L. (Xiangfei Liu); validation X.W., X.L. (Xueyang Li) and L.Y.; formal analysis, B.N.; investigation, J.H., X.L. (Xiangfei Liu), X.W. and X.L. (Xueyang Li); resources, B.N.; data curation, X.L. (Xueyang Li) and L.Y.; writing—original draft, J.H., X.L. (Xiangfei Liu), X.W. and B.N.; writing—review and editing, J.H., X.L. (Xiangfei Liu) and B.N.; visualization, L.Y.; supervision, B.N.; project administration, B.N.; funding acquisition, B.N. All authors have read and agreed to the published version of the manuscript.

**Funding:** This research was funded by the Collaborative Innovation Center for Emissions Trading System Co-constructed by the Province and Ministry (23CICETS-YB015).

**Data Availability Statement:** The raw data supporting the conclusions of this article will be made available by the authors on request.

**Acknowledgments:** The authors would like to thank the editors and reviewers for their helpful comments.

**Conflicts of Interest:** The authors declare no conflicts of interest.

## References

1. Arneth, A.; Sitch, S.; Pongratz, J.; Stocker, B.D.; Ciais, P.; Poulter, B.; Bayer, A.D.; Bondeau, A.; Calle, L.; Chini, L.P.; et al. Historical Carbon Dioxide Emissions Caused by Land-Use Changes Are Possibly Larger than Assumed. *Nat. Geosci.* **2017**, *10*, 79–84. [\[CrossRef\]](#)
2. Piao, S.; Huang, M.; Liu, Z.; Wang, X.; Ciais, P.; Canadell, J.G.; Wang, K.; Bastos, A.; Friedlingstein, P.; Houghton, R.A.; et al. Lower Land-Use Emissions Responsible for Increased Net Land Carbon Sink during the Slow Warming Period. *Nat. Geosci.* **2018**, *11*, 739–743. [\[CrossRef\]](#)
3. Searchinger, T.D.; Wierseni, S.; Beringer, T.; Dumas, P. Assessing the Efficiency of Changes in Land Use for Mitigating Climate Change. *Nature* **2018**, *564*, 249–253. [\[CrossRef\]](#)
4. Mahmood, H.; Alkhateeb, T.T.Y.; Furqan, M. Industrialization, Urbanization and CO<sub>2</sub> Emissions in Saudi Arabia: Asymmetry Analysis. *Energy Rep.* **2020**, *6*, 1553–1560. [\[CrossRef\]](#)
5. The Intergovernmental Panel on Climate Change Climate Change 2022: Mitigation of Climate Change. Available online: <https://www.ipcc.ch/report/sixth-assessment-report-working-group-3/> (accessed on 10 September 2023).
6. Qin, Z.; Zhu, Y.; Canadell, J.G.; Chen, M.; Li, T.; Mishra, U.; Yuan, W. Global Spatially Explicit Carbon Emissions from Land-Use Change over the Past Six Decades (1961–2020). *One Earth* **2024**, *7*, 835–847. [\[CrossRef\]](#)
7. Wang, D.; Fu, J.; Xie, X.; Ding, F.; Jiang, D. Spatiotemporal Evolution of Urban-Agricultural-Ecological Space in China and Its Driving Mechanism. *J. Clean. Prod.* **2022**, *371*, 133684. [\[CrossRef\]](#)
8. Mishra, A.; Humpenöder, F.; Churkina, G.; Reyer, C.P.O.; Beier, F.; Bodirsky, B.L.; Schellnhuber, H.J.; Lotze-Campen, H.; Popp, A. Land Use Change and Carbon Emissions of a Transformation to Timber Cities. *Nat. Commun.* **2022**, *13*, 4889. [\[CrossRef\]](#)
9. Zhao, L.; Zhang, C.; Wang, Q.; Yang, C.; Suo, X.; Zhang, Q. Climate Extremes and Land Use Carbon Emissions: Insight from the Perspective of Sustainable Land Use in the Eastern Coast of China. *J. Clean. Prod.* **2024**, *452*, 142219. [\[CrossRef\]](#)
10. Friedlingstein, P.; O’Sullivan, M.; Jones, M.W.; Andrew, R.M.; Bakker, D.C.E.; Hauck, J.; Landschützer, P.; Quéré, C.L.; Luijkx, I.T.; Peters, G.P.; et al. Global Carbon Budget 2023. *Earth Syst. Sci. Data* **2023**, *15*, 5301–5369. [\[CrossRef\]](#)
11. Obermeier, W.A.; Schwingshackl, C.; Bastos, A.; Conchedda, G.; Gasser, T.; Grassi, G.; Houghton, R.A.; Tubiello, F.N.; Sitch, S.; Pongratz, J. Country-Level Estimates of Gross and Net Carbon Fluxes from Land Use, Land-Use Change and Forestry. *Earth Syst. Sci. Data* **2024**, *16*, 605–645. [\[CrossRef\]](#)
12. Duffy, C.; Prudhomme, R.; Duffy, B.; Gibbons, J.; Iannetta, P.P.M.; O’Donoghue, C.; Ryan, M.; Styles, D. Randomized National Land Management Strategies for Net-Zero Emissions. *Nat. Sustain.* **2022**, *5*, 973–980. [\[CrossRef\]](#)
13. Hartung, K.; Bastos, A.; Chini, L.; Ganzenmüller, R.; Havermann, F.; Hurtt, G.C.; Loughran, T.; Nabel, J.E.M.S.; Nützel, T.; Obermeier, W.A.; et al. Bookkeeping Estimates of the Net Land-Use Change Flux—A Sensitivity Study with the CMIP6 Land-Use Dataset. *Earth Syst. Dynam.* **2021**, *12*, 763–782. [\[CrossRef\]](#)
14. Liu, H.; Yin, W.; Yan, F.; Cai, W.; Du, Y.; Wu, Y. A Coupled STIRPAT-SD Model Method for Land-Use Carbon Emission Prediction and Scenario Simulation at the County Level. *Environ. Impact Assess. Rev.* **2024**, *108*, 107595. [\[CrossRef\]](#)



15. Yang, F.; He, F.; Li, S.; Li, M.; Wu, P. A New Estimation of Carbon Emissions from Land Use and Land Cover Change in China over the Past 300 Years. *Sci. Total Environ.* **2023**, *863*, 160963. [\[CrossRef\]](#)
16. Jing, X.; Tian, G.; He, Y.; Wang, M. Spatial and Temporal Differentiation and Coupling Analysis of Land Use Change and Ecosystem Service Value in Jiangsu Province. *Ecol. Indic.* **2024**, *163*, 112076. [\[CrossRef\]](#)
17. Wang, Q.; Yang, C.; Wang, M.; Zhao, L.; Zhao, Y.; Zhang, Q.; Zhang, C. Decoupling Analysis to Assess the Impact of Land Use Patterns on Carbon Emissions: A Case Study in the Yellow River Delta Efficient Eco-Economic Zone, China. *J. Clean. Prod.* **2023**, *412*, 137415. [\[CrossRef\]](#)
18. Crivelari-Costa, P.M.; Lima, M.; La Scala, N., Jr.; Rossi, F.S.; Della-Silva, J.L.; Dalagnol, R.; Teodoro, P.E.; Teodoro, L.P.R.; Oliveira, G.D.; Junior, J.F.D.O.; et al. Changes in Carbon Dioxide Balance Associated with Land Use and Land Cover in Brazilian Legal Amazon Based on Remotely Sensed Imagery. *Remote Sens.* **2023**, *15*, 2780. [\[CrossRef\]](#)
19. Fan, M.; Wang, Z.; Xue, Z. Spatiotemporal Evolution Characteristics, Influencing Factors of Land Use Carbon Emissions, and Low-Carbon Development in Hubei Province, China. *Ecol. Inform.* **2024**, *81*, 102567. [\[CrossRef\]](#)
20. Riahi, K.; Van Vuuren, D.P.; Kriegler, E.; Edmonds, J.; O'Neill, B.C.; Fujimori, S.; Bauer, N.; Calvin, K.; Dellink, R.; Fricko, O.; et al. The Shared Socioeconomic Pathways and Their Energy, Land Use, and Greenhouse Gas Emissions Implications: An Overview. *Glob. Environ. Chang.* **2017**, *42*, 153–168. [\[CrossRef\]](#)
21. Li, L.; Huang, X.; Yang, H. Optimizing Land Use Patterns to Improve the Contribution of Land Use Planning to Carbon Neutrality Target. *Land. Use Policy* **2023**, *135*, 106959. [\[CrossRef\]](#)
22. Rong, T.; Zhang, P.; Zhu, H.; Jiang, L.; Li, Y.; Liu, Z. Spatial Correlation Evolution and Prediction Scenario of Land Use Carbon Emissions in China. *Ecol. Inform.* **2022**, *71*, 101802. [\[CrossRef\]](#)
23. Zhang, Z.; Yu, X.; Hou, Y.; Chen, T.; Lu, Y.; Sun, H. Carbon Emission Patterns and Carbon Balance Zoning in Urban Territorial Spaces Based on Multisource Data: A Case Study of Suzhou City, China. *ISPRS Int. J. Geo-Inf.* **2023**, *12*, 385. [\[CrossRef\]](#)
24. Liu, Y.; Zhou, Y. Territory Spatial Planning and National Governance System in China. *Land. Use Policy* **2021**, *102*, 105288. [\[CrossRef\]](#)
25. Li, X.; Wang, Y.; Wu, K.; Feng, Z. Analysis and Prediction of Carbon Balance in Production-Living-Ecological Space of Henan Province, China. *Environ. Sci. Pollut. Res.* **2023**, *30*, 75973–75988. [\[CrossRef\]](#)
26. Xiong, S.; Yang, F.; Li, J.; Xu, Z.; Ou, J. Temporal-Spatial Variation and Regulatory Mechanism of Carbon Budgets in Territorial Space through the Lens of Carbon Balance: A Case of the Middle Reaches of the Yangtze River Urban Agglomerations, China. *Ecol. Indic.* **2023**, *154*, 110885. [\[CrossRef\]](#)
27. Fu, B.; Wu, M.; Che, Y.; Yang, K. Effects of Land-Use Changes on City-Level Net Carbon Emissions Based on a Coupled Model. *Carbon Manag.* **2017**, *8*, 245–262. [\[CrossRef\]](#)
28. Cao, W.; Yuan, X. Region-County Characteristic of Spatial-Temporal Evolution and Influencing Factor on Land Use-Related CO<sub>2</sub> Emissions in Chongqing of China, 1997–2015. *J. Clean. Prod.* **2019**, *231*, 619–632. [\[CrossRef\]](#)
29. Yan, H.; Guo, X.; Zhao, S.; Yang, H. Variation of Net Carbon Emissions from Land Use Change in the Beijing-Tianjin-Hebei Region during 1990–2020. *Land* **2022**, *11*, 997. [\[CrossRef\]](#)
30. Li, S.; Liu, Y.; Wei, G.; Bi, M.; He, B.-J. Carbon Surplus or Carbon Deficit under Land Use Transformation in China? *Land. Use Policy* **2024**, *143*, 107218. [\[CrossRef\]](#)
31. Zhang, Y.; Linlin, X.; Weining, X. Analyzing Spatial Patterns of Urban Carbon Metabolism: A Case Study in Beijing, China. *Landsc. Urban. Plan.* **2014**, *130*, 184–200. [\[CrossRef\]](#)
32. Yang, Y.; Li, H. Spatiotemporal Dynamic Decoupling States of Eco-Environmental Quality and Land-Use Carbon Emissions: A Case Study of Qingdao City, China. *Ecol. Inform.* **2023**, *75*, 101992. [\[CrossRef\]](#)
33. Bian, R.; Chen, J.; Zhang, T.; Gao, C.; Niu, Y.; Sun, Y.; Zhan, M.; Zhao, F.; Zhang, G. Influence of the Classification of Municipal Solid Wastes on the Reduction of Greenhouse Gas Emissions: A Case Study of Qingdao City, China. *J. Clean. Prod.* **2022**, *376*, 134275. [\[CrossRef\]](#)
34. Wu, C.B.; Huang, G.H.; Liu, Z.P.; Zhen, J.L.; Yin, J.G. Scenario Analysis of Carbon Emissions' Anti-Driving Effect on Qingdao's Energy Structure Adjustment with an Optimization Model, Part II: Energy System Planning and Management. *J. Environ. Manag.* **2017**, *188*, 120–136. [\[CrossRef\]](#) [\[PubMed\]](#)
35. Zhao, S.; Duan, W.; Zhao, D.; Song, Q. Identifying the Influence Factors of Residents' Low-Carbon Behavior under the Background of "Carbon Neutrality": An Empirical Study of Qingdao City, China. *Energy Rep.* **2022**, *8*, 6876–6886. [\[CrossRef\]](#)
36. Hu, Q.; Zhang, Z.; Niu, L. Identification and Evolution of Territorial Space from the Perspective of Composite Functions. *Habitat. Int.* **2022**, *128*, 102662. [\[CrossRef\]](#)
37. Chuai, X.; Huang, X.; Wang, W.; Zhao, R.; Zhang, M.; Wu, C. Land Use, Total Carbon Emissions Change and Low Carbon Land Management in Coastal Jiangsu, China. *J. Clean. Prod.* **2015**, *103*, 77–86. [\[CrossRef\]](#)
38. IPCC 2019 Refinement to the 2006 IPCC Guidelines for National Greenhouse Gas Inventory. 2019. Available online: <https://www.ipcc.ch/report/2019-refinement-to-the-2006-ipcc-guidelines-for-national-greenhouse-gas-inventories/> (accessed on 10 September 2023).
39. Li, W.; Chen, Z.; Li, M.; Zhang, H.; Li, M.; Qiu, X.; Zhou, C. Carbon Emission and Economic Development Trade-Offs for Optimizing Land-Use Allocation in the Yangtze River Delta, China. *Ecol. Indic.* **2023**, *147*, 109950. [\[CrossRef\]](#)
40. Zhao, J.; Zhao, Y.; Yang, X. Evolution Characteristics and Driving Mechanism of the Territorial Space Pattern in the Yangtze River Economic Belt, China. *Land* **2022**, *11*, 1447. [\[CrossRef\]](#)

41. Lefever, D.W. Measuring Geographic Concentration by Means of the Standard Deviation Ellipse. *Am. J. Sociol.* **1926**, *32*, 88–94. [\[CrossRef\]](#)
42. Gui, D.; He, H.; Liu, C.; Han, S. Spatio-Temporal Dynamic Evolution of Carbon Emissions from Land Use Change in Guangdong Province, China, 2000–2020. *Ecol. Indic.* **2023**, *156*, 111131. [\[CrossRef\]](#)
43. Duman, Z.; Mao, X.; Cai, B.; Zhang, Q.; Chen, Y.; Gao, Y.; Guo, Z. Exploring the Spatiotemporal Pattern Evolution of Carbon Emissions and Air Pollution in Chinese Cities. *J. Environ. Manag.* **2023**, *345*, 118870. [\[CrossRef\]](#) [\[PubMed\]](#)
44. Jia, Q.; Yin, Z. Land Spatial Evolution and Ecosystem Response of Coastal Cities Based on Ecological-Production-Living Function: A Case Study in Qingdao City, Shandong Province. *Geomat. Spat. Inf. Technol.* **2023**, *46*, 12–16.
45. Li, X.; Lei, L.; Li, J. Integrating Ecosystem Service Value into the Evaluation of Sustainable Land Use in Fast-Growing Cities: A Case Study of Qingdao, China. *Ecol. Indic.* **2023**, *153*, 110434. [\[CrossRef\]](#)
46. Wang, Z.; Liu, D.; Wang, M.; Yu, Y. Coastal Urban Expansion and Its Eco-Environmental Effects Using Multi-Source Data. *Geospat. Inf.* **2024**, *22*, 49–53.
47. Zhang, P.; Zhou, Y.; Luan, K.; Jia, B. Spatiotemporal Evolution and Driving Factors of Carbon Emissions in Qingdao City Based on GeoDetector. *Glob. NEST J.* **2023**, *25*, 170–177.
48. Liu, S.; Xiao, W.; Ye, Y.; He, T.; Luo, H. Rural Residential Land Expansion and Its Impacts on Cultivated Land in China between 1990 and 2020. *Land Use Policy* **2023**, *132*, 106816. [\[CrossRef\]](#)
49. Shan, Y.; Liu, J.; Liu, Z.; Shao, S.; Guan, D. An Emissions-Socioeconomic Inventory of Chinese Cities. *Sci. Data* **2019**, *6*, 190027. [\[CrossRef\]](#)
50. Hasan, A.S.M.M.; Trianni, A. Boosting the Adoption of Industrial Energy Efficiency Measures through Industry 4.0 Technologies to Improve Operational Performance. *J. Clean. Prod.* **2023**, *425*, 138597. [\[CrossRef\]](#)
51. Shang, W.-L.; Ling, Y.; Ochieng, W.; Yang, L.; Gao, X.; Ren, Q.; Chen, Y.; Cao, M. Driving Forces of CO<sub>2</sub> Emissions from the Transport, Storage and Postal Sectors: A Pathway to Achieving Carbon Neutrality. *Appl. Energy* **2024**, *365*, 123226. [\[CrossRef\]](#)
52. Ji, M.; Li, J.; Zhang, M. What Drives the Agricultural Carbon Emissions for Low-Carbon Transition? Evidence from China. *Environ. Impact Assess. Rev.* **2024**, *105*, 107440. [\[CrossRef\]](#)
53. Xu, X. Investigating the Impacts of Three-Dimensional Spatial Structures on CO<sub>2</sub> Emissions at the Urban Scale. *Sci. Total Environ.* **2021**, *762*, 143096. [\[CrossRef\]](#) [\[PubMed\]](#)
54. Leibowicz, B.D. Effects of Urban Land-Use Regulations on Greenhouse Gas Emissions. *Cities* **2017**, *70*, 135–152. [\[CrossRef\]](#)
55. Liu, J.; Peng, K.; Zuo, C.; Li, Q. Spatiotemporal Variation of Land-Use Carbon Emissions and Its Implications for Low Carbon and Ecological Civilization Strategies: Evidence from Xiamen-Zhangzhou-Quanzhou Metropolitan Circle, China. *Sustain. Cities Soc.* **2022**, *86*, 104083. [\[CrossRef\]](#)
56. Tian, Y.; Zhang, J.; Li, B. Agricultural carbon emissions in China: Calculation, spatial-temporal comparison and decoupling effects. *Resour. Sci.* **2012**, *34*, 2097–2105. (In Chinese)
57. Wu, X.; Zhang, J.; Tian, Y. Provincial agricultural carbon emissions in China: Calculation, performance change and influencing factors. *Resour. Sci.* **2014**, *36*, 129–138. (In Chinese)
58. Qu, Y. *The Research on Carbon Flux Calculation, Carbon Emission Effects and Regulation Mechanism of Wuhan Land Use*; Huazhong Agricultural University: Wuhan, China, 2015. (In Chinese)
59. Long, Z. *Spatiotemporal Pattern of Carbon Emissions and Carbon Balance Zoning Optimization in the County Scale*; Lanzhou University: Lanzhou, China, 2022. (In Chinese)
60. Fang, J.; Guo, Z.; Piao, S. Estimation of carbon sinks in terrestrial vegetation in China from 1981 to 2000. *Sci. Sin.* **2007**, *6*, 804–812. (In Chinese)
61. Zhang, J.; Zhang, A.; Dong, J. Carbon emission effects of land use and Influencing factors decomposition of carbon emissions in Wuhan urban agglomeration. *Resour. Environ. Yangtze Basin* **2014**, *23*, 595–602. (In Chinese)
62. Duan, X.; Wang, X.; Lu, F.; Ouyang, Z.Y. Carbon sequestration and its potential by wetland ecosystems in China. *Acta Ecol. Sin.* **2008**, *28*, 463–469. (In Chinese)

**Disclaimer/Publisher’s Note:** The statements, opinions and data contained in all publications are solely those of the individual author(s) and contributor(s) and not of MDPI and/or the editor(s). MDPI and/or the editor(s) disclaim responsibility for any injury to people or property resulting from any ideas, methods, instructions or products referred to in the content.